Clinical Impact of Combination of Scatter, Attenuation Correction, and Depth-Dependent Resolution Recovery for ^{201}Tl Studies

François Harel, Rémi Génin, Doumit Daou, Rachida Lebtahi, Nicolas Delahaye, Badia O. Helal, Dominique Le Guludec, and Marc Faraggi

Department of Nuclear Medicine, Bichat Hospital, Assistance Publique Hôpitaux de Paris, Paris; and Department of Nuclear Medicine, Antoine Béclère Hospital, Assistance Publique Hôpitaux de Paris, Clamart, France

A lack of specificity for myocardial perfusion imaging has been widely reported, mostly related to false-positive defects on the inferior wall. The application of depth-dependent resolution recovery (RR), attenuation correction (AC) using external source devices, and scatter correction has been proposed to resolve this pitfall. **Methods:** We studied the clinical benefit of depth-dependent RR, nonuniform AC using a scanning line source, and scatter correction (photon energy recovery [PER]) compared with filtered backprojection alone. Eighty-two patients were included: 40 healthy volunteers with a low likelihood of coronary artery disease (control group) and 42 patients with proven right or circumflex coronary artery disease but without involvement of the left anterior descending artery. Among these 82 patients, the images of 33 were also processed with PER. **Results:** RR did not alter the performance of filtered backprojection alone. AC + RR greatly improved specificity and the rate of normal ^{201}Tl SPECT findings in the control population (from 56% to 95% and from 53% to 100%, respectively) but significantly decreased sensitivity (from 92% to 54%). AC + RR generated a false anteroapical defect in 21% of patients and reverse redistribution of the apex in 23%. AC + RR significantly decreased the extent of the stress defect (from 4.09 to 3.21 segments, $P < 0.003$) and increased the perfusion score of the stress defect (from 0.78 ± 0.72 to 1.47 ± 1.11, $P < 0.00061$). Moreover, AC + RR generated overcorrection on the inferior wall, leading to false estimation of viability for 11 of 15 patients with an old inferior myocardial scar without evidence of residual viability. PER decreased overcorrection on the inferior wall, but without improving sensitivity. PER did not significantly reduce the number of anteroapical false-positives or the number of apical reverse distribution cases. **Conclusion:** AC + RR improved the specificity and normalcy rate of ^{201}Tl SPECT myocardial perfusion imaging but generated overcorrection on the inferior wall, leading to low sensitivity and to false evaluation of myocardial viability in 73% of the patients with inferior infarction. AC + RR also generated anteroapical artifacts. The addition of scatter correction did not significantly reduce these drawbacks.

Key Words: attenuation correction; scatter correction; myocardial perfusion

J Nucl Med 2001; 42:1451–1456

Received Jan. 16, 2001; revision accepted Jun. 12, 2001.

For correspondence or reprints contact: François Harel, MD, Department of Nuclear Medicine, Bichat Hospital, AP-HP, 46 rue Henri Huchard, 75877 Paris CEDEX 18, France.

One of the most frequently used techniques for noninvasive myocardial perfusion imaging (MPI) is SPECT. Although MPI has been shown accurate in the diagnosis of coronary artery disease (CAD), a lack of specificity has been widely reported, mostly related to false-positive defects on the inferior wall (*1*). This phenomenon is created by a loss in depth-dependent resolution and by attenuation of the signal. Therefore, depth-dependent resolution recovery (RR) software programs have been proposed to improve filtered backprojection (FBP) reconstruction of SPECT images. For attenuation correction (AC), the most conceptually interesting procedure should be based on evaluation of an attenuation map (μ-map) using an external source for acquisition of transmission images, this procedure being often performed for PET studies (*2*). The impact of these procedures on the final scintigraphic reports is expected to be major. First, enhancement of specificity for detecting CAD related to the inferior wall (and therefore involving the right coronary artery [RC] or circumflex coronary artery [Cx]), without a decrease in sensitivity, is expected. Second, we expect these corrections to avoid the generation of anterior or apical artifacts in patients free from disease of the left anterior descending coronary artery (LAD). Third, the impact of these methods on the measurement of proven prognostic factors (i.e., the size and depth of the tracer defect) has to be evaluated (*3–5*). For this purpose, patients with proven previous Q-wave inferior myocardial infarction, a coronary artery with an infarct-related chronic occlusion, and a thin and bright akinetic inferior wall on 2-dimensional echocardiography offer a convenient model for evaluating the alteration of these measurements within the area at risk.

The goal of this study was to determine the clinical impact of the simultaneous use of nonuniform AC with a scanning line source and of depth-dependent RR. First, we evaluated the effect of depth-dependent RR when added to simple FBP. Then, we compared an AC + RR combination with an FBP + RR combination in 2 groups of subjects. One was a control group with a low likelihood of CAD, and

the other was a population with proven RC or Cx disease but no LAD disease. Selected patients with old inferior myocardial infarction fulfilling the inclusion criteria were also included. A third goal was the evaluation of the additional benefit of scatter correction (photon energy recovery [PER]) in a subset of the global population.

MATERIALS AND METHODS

Study Population

Two groups of subjects were selected between January 1999 and December 1999. Group A (control group, $n = 40$) included healthy volunteers with a low likelihood of CAD (no history of CAD, 0 or 1 risk factor, and negative findings on electrocardiography stress testing) (*6*) or with absence of significant lesions on coronary angiography. Group B ($n = 42$) included patients referred for detection of myocardial ischemia. To be included in group B, patients had to have chronic RC or Cx disease (stenosis $>$ 70%) without significant involvement of the LAD (stenosis $<$ 50%), as shown by coronary angiography performed within 3 mo before the SPECT study. Also included were patients with previous old ($>$3 mo) inferior infarction if they presented with Q-wave infarction, an occluded infarct-related artery without collateral blood flow on coronary angiography, and a thin ($<$6 mm) and bright akinetic inferior wall on 2-dimensional echocardiography. We excluded patients with unstable angina; CAD involving the left main, left anterior, or diagonal coronary artery; previous anterior myocardial infarction; or previous inferior myocardial infarction that did not fulfill the inclusion criteria. Also excluded were patients with unsatisfactory acquisitions and patients unwilling to participate in the study. Informed consent was obtained from each patient, and the ethics committee of our institution approved the protocol.

In group B, 34 patients (81%) had 1-vessel disease (25 patients with RC disease and 9 with Cx disease), and the remaining 8 patients (19%) had RC and Cx disease. Fifteen patients had inferior infarction without evidence of myocardial viability.

Acquisition of Clinical Data

For all the studies, quality control was performed by examination of the rotating projections and sinograms. Acquisitions that were inadequate because of undesirable subject motion were rejected ($n = 3$).

SPECT was performed 10 min and 4 h after injection of the tracer at peak exercise. The stress test consisted of exercise on an ergonomic bicycle for subjects who could reach at least 85% of the age-predicted maximal heart rate ($n = 49$). For the other subjects ($n = 31$), we used a combined test comprising a standard infusion of 0.80 mg/kg dipyridamole, for a maximal dose of 70 mg over 4 min, and a Bruce exercise protocol using a steady bicycle (*7*). Two subjects could not exercise and a dipyridamole test alone was used. After injection of 111–150 MBq ^{201}Tl-chloride, imaging was performed using a 90° double-head camera (DST; SMV International, Buc, France) equipped with low-energy, high-resolution parallel-hole collimators. All tests were performed after withdrawal of antianginal treatment. The subjects were supine, and the heart was in the center of the orbit of the rotating camera. The acquisition parameters were as follows: no acquisition zoom, 32 projections over a 180° orbit, and a 64 × 64 matrix in 16-bit mode. For each projection, 50 s of emission data were first acquired, followed by 12 s of transmission data. Energy windowing was performed with a 20% window centered on 70 keV. Among the 82 subjects, the data of 33 (7 in group A and 26 in group B) were also corrected for photon scattering using a method of spectral deconvolution (PER) with 6 windows of energy (50–55, 55–60, 60–65, 65–69, 69–74, and 74–81 keV) (*8*).

For transmission images, 2 external shuttered scanning line sources (11 GBq ^{153}Gd) were used. These sources were collimated with lead shielding to produce a planar beam that yields transmission CT images. The shield door was closed during the emission acquisition to avoid downscatter of transmission-source photons into the emission data (*9*). These images were used to calculate the μ-map after normalization to a reference scan and logarithmic inversion.

Processing of Clinical Data

All software processing was performed with Vision, version 5.0 (SMV International). The ^{201}Tl emission data were first corrected for the depth-dependent resolution of the collimator with an inverted-filter method (deconvolution) using a roll-off boost point of 1.4 (*10,11*). These corrected emission data were then used as input for reconstruction processing with a modified Chang iterative algorithm (7 iterations) incorporating the μ-map (*12,13*). For the subgroup of scatter-corrected acquisitions ($n = 33$), the correction based on PER was applied to the raw projections before AC + RR (*8*). For patients with previous myocardial infarction, tracer uptake and defect size were analyzed using bull's-eye polar maps (*14*).

Scintigraphic Interpretation of Clinical Data

SPECT data obtained from the CAD and control groups were mixed and read by 2 independent trained observers. The observers were unaware of the group to which the subject belonged and, therefore, of the angiographic results. Perfusion was evaluated using a 13-region cardiac segmentation (Fig. 1). The perfusion score was calculated by summing the perfusion scores of the 13 segments (0 for no uptake to 3 for normal perfusion) and dividing by the number of involved segments. This score reflected the

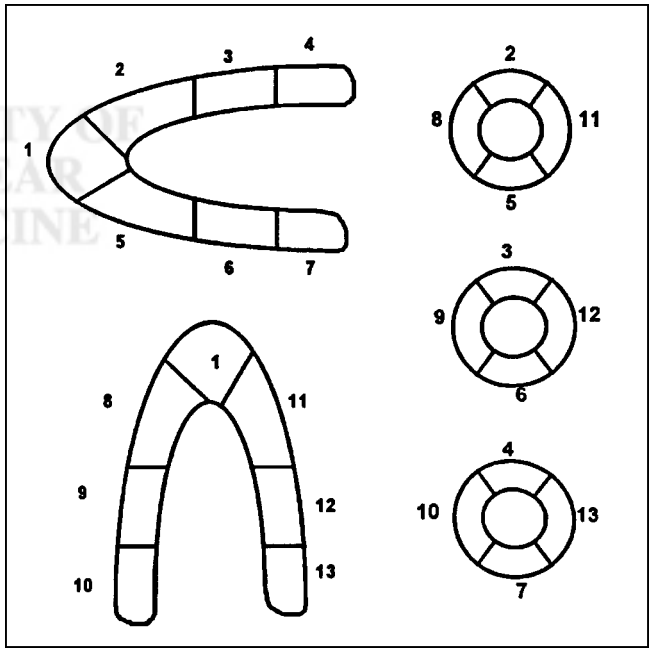

FIGURE 1. Myocardial segmentation in 13 segments.

SOCIETY OF NUCLEAR MEDICINE

TABLE 1
Stress Studies

Finding	Group A	Group B	*P*
n	40	42	
Age (y)	51 ± 15	59 ± 11	0.04
Ergonomic bicycle alone	29	20	
Dipyridamole alone	1	1	
Combined stress studies	10	21	
Clinically positive	0	6	0.013
Electrically positive	1	12	0.002
Electrically equivocal	4	0	
Peak work load (W)	139 ± 67	107 ± 42	0.036
Peak heart rate (% maximum)	88 ± 14	74 ± 15	0.0002

severity of the defects. The extent of a defect was expressed as the number of abnormal segments. For patients with previous myocardial infarction, a bull's-eye polar map was generated. Tracer uptake within the infarct area was computed as the ratio of the average total counts per pixel within the abnormal area to the average total counts per pixel within a reference area drawn on the anterior wall. The percentage of uptake was compared with a threshold value of 60%, which is usually used in our laboratory to define myocardial viability (*15*).

The data corrected with the various techniques—standard reconstruction (FBP using a Hanning filter, 0.34 cycles per centimeter) with no other correction ($n = 82$), standard reconstruction after correction with RR (FBP + RR, $n = 82$), AC + RR ($n = 82$), and PER + AC + RR ($n = 33$)—were interpreted in random order.

Final Diagnosis of CAD

After SPECT interpretation, the final diagnosis was based on the angiographic results. Stenosis was considered significant if the diameter of the coronary artery was narrowed by ≥70%. Hypofixation of the lateral wall was considered to be related to Cx involvement, and inferior wall abnormalities were considered to be related to RC or Cx involvement, according to the coronary angiography data. Sensitivity, specificity, accuracy, and normalcy (defined as the rate of normal ^{201}Tl SPECT findings in the control population) of all datasets (FBP, FBP + RR, AC + RR, and PER + AC + RR) were computed for the lateral and inferior walls, and the number of anterior or apical artifacts was reported.

Statistical Analysis

Statistical calculations were performed using Prophet, version 5.0 (BBN Systems and Technologies, Cambridge, MA). Data were expressed as mean ± SD. The extent and severity of the defects were compared using a paired 2-sample Wilcoxon signed rank test (2-tailed) or a Friedman test, as required. The numbers of segments with normal or abnormal uptake were compared qualitatively with a χ^2 test. $P < 0.05$ was considered significant.

RESULTS

The results of the stress studies and of ^{201}Tl SPECT for the 82 patients are presented in Tables 1 and 2. For detecting RC or Cx disease, the uncorrected reconstruction (FBP) had a sensitivity of 92% and a specificity of 56%. The normalcy rate for FBP was 53%. All patients with an area of scarring from a previous myocardial infarction had a resting ^{201}Tl uptake of <60% in that area.

When compared with FBP alone, the addition of RR to FBP did not significantly change the sensitivity, specificity, or accuracy of MPI or the number of created artifacts. The extent and severity of defects were not altered. Because diagnostic performances were unchanged, we therefore combined AC and RR for the processing of clinical data.

The combination AC + RR improved tracer uptake in the inferior wall of subjects free of CAD but decreased the number of abnormal SPECT findings in patients with RC or Cx disease. When AC was added to RR, no inferior defect was found in group A whereas 21 group B patients had an abnormal SPECT finding. By comparison, when FBP was used, 19 inferior defects were found in group A and 36 were found in group B ($P < 0.001$). Therefore, the normalcy rate increased from 53% to 100% when AC + RR was used. Conversely, normal inferior uptake was found in 40 of 40 group A subjects and in 18 of 42 group B patients when AC + RR was used, compared with 21

SOCIETY OF NUCLEAR MEDICINE

TABLE 2
Detection of Inferior or Circumflex Involvement

Finding	PER + AC + RR (*n* = 33)	AC + RR (*n* = 82)	FBP + RR (*n* = 82)	FBP (*n* = 82)
Sensitivity (%)	67	54	97	92
Specificity (%)	75	95	50	56
Accuracy (%)	69	76	73	73
Normalcy rate (%)	75	100	53	53
Anteroapical false-positive defect (*n*,%)	13 (39%)	17 (21%)	1 (1%)	1 (1%)
Apical reverse redistribution (*n*,%)	7 (21%)	19 (23%)	0 (0%)	0 (0%)
Extent of stress defect (segments)	3.60 ± 2.14	3.21 ± 2.40*	4.06 ± 1.58	4.09 ± 1.57
Extent of rest defect (segments)	2.44 ± 1.92*†	2.23 ± 2.17*	2.65 ± 1.66	3.26 ± 1.69
Perfusion score in stress defect	1.41 ± 0.93*†	1.47 ± 1.11*	0.55 ± 0.82	0.78 ± 0.72
Perfusion score in rest defect	1.71 ± 1.02*	1.62 ± 0.99*	1.27 ± 1.06	1.38 ± 0.87

*$P < 0.05$ compared with FBP.
†$P < 0.05$ compared with AC + RR.

TABLE 3
Tracer Uptake in Patients with Inferior Myocardial Infarction

Finding	PER + AC + RR	AC + RR	FBP
Extent of infarcted area (%)	10.4 ± 7.1	7.8 ± 7.1*	13.4 ± 4.5
Perfusion score in infarcted area (%)	59.4 ± 19.5†	72.3 ± 16.6*	52.6 ± 6.0

*$P < 0.05$ compared with FBP.
†$P < 0.05$ compared with AC + RR.

and 3, respectively, for FBP. Therefore, AC + RR improved specificity from 56% to 95% but dramatically decreased sensitivity from 92% to 54% (Table 2). The stress defect extent obtained with FBP decreased from 4.09 ± 1.57 to 3.21 ± 2.40 segments ($P = 0.003$) and the perfusion score during stress increased from 0.78 ± 0.72 to 1.47 ± 1.11 ($\Delta = 88\%$; $P = 0.00006$) when AC + RR was used. This trend was particularly noticeable in selected patients who had previous myocardial infarction ($n = 15$), in whom AC + RR decreased the extent of the defect from 13.4% ± 4.5% of the bull's-eye surface to 7.8% ± 7.1% ($P = 0.003$) and increased the estimation of tracer uptake from 52.6% ± 6% to 72.3% ± 16.6% ($P = 0.001$; Table 3). In 11 (73%) of these 15 patients without evidence of residual myocardial viability, the algorithm increased this uptake to a level that could lead to a false-positive diagnosis of myocardial viability on the basis of ^{201}Tl SPECT data (Fig. 2).

Furthermore, AC + RR induced false-positive scans in the anterior or apical area, whereas no patients had significant involvement of the LAD. Specifically, 17 anteroapical defects and 19 reverse-redistribution changes in the apical area (defects appearing only at rest when the LAD was free of disease as required by inclusion criteria) were observed with AC + RR.

Additional scatter correction was applied in 33 subjects (7 in group A and 26 in group B, including 7 with inferior myocardial infarction). Sensitivity and specificity were 67% and 75%, respectively, for AC + RR + PER. Although the addition of PER did not dramatically alter sensitivity when compared with AC + RR, the extent of the defect and the perfusion scores tended to be restored to the values obtained with FBP ($P = 0.01$ for stress defect perfusion score; Table 2). Compared with AC + RR, adding PER reduced the number of patients with previous inferior myocardial infarction and apparent ^{201}Tl uptake > 60% from 11 of 15 (73%) to 2 of 7 (29%). Figure 3 shows the improvement in inferior overcorrection induced by PER, and Figure 4 displays the associated bull's-eye polar maps.

DISCUSSION

Inferior artifacts caused by the attenuation of γ-rays created by soft tissue are known to impair the accuracy of SPECT (*16,17*). Besides uniform correction of attenuation that does not take into account the heterogeneity of tissue density (*13,18*), transmission techniques for evaluating the thoracic μ-map seem promising (*19–26*). To evaluate such correction methods, most of the previous investigations enrolled a general population of patients with multivessel CAD, without exclusively controlling for RC and Cx involvement (*27,28*). Because both the generation of unexpected anterior artifacts and a decrease in sensitivity should be avoided, we deliberately chose to focus on inferior wall abnormalities, excluding LAD involvement but including a

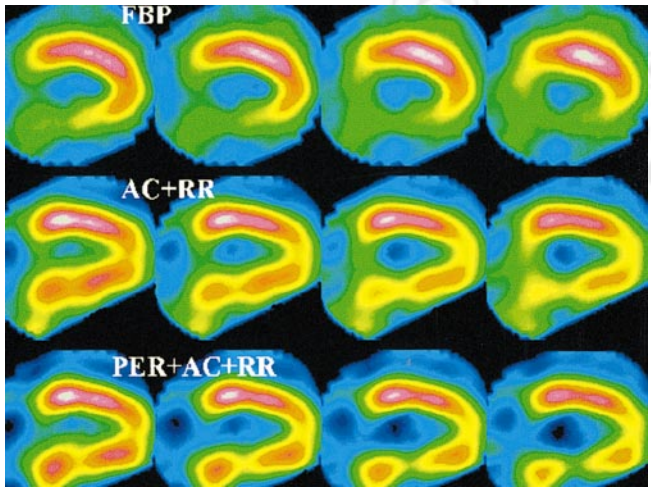

FIGURE 2. Vertical long-axis slices from exercise study on patient with old inferior infarction and normal LAD. Top shows images obtained with FBP, middle shows false apical defect created by AC + RR, and bottom shows that PER does not significantly correct this false defect.

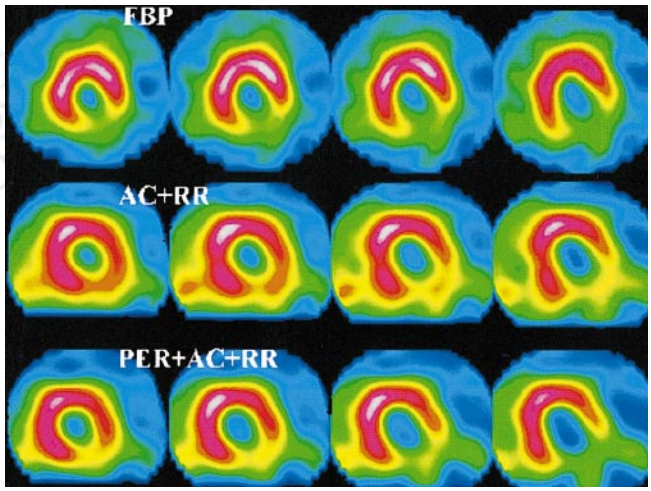

FIGURE 3. Short-axis slices from rest study on patient with old inferior infarction and no evidence of residual myocardial viability. Inferior uptake obtained with FBP (top) is excessively enhanced by AC + RR (middle) and partially restored with PER (bottom).

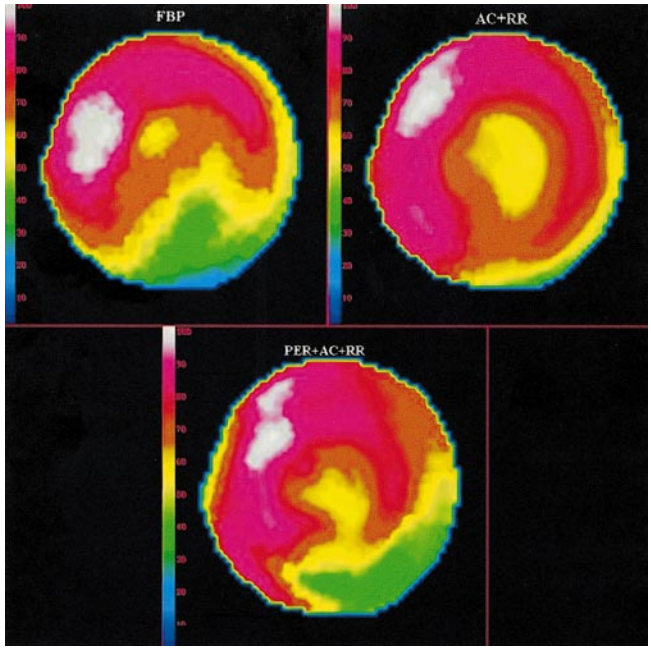

FIGURE 4. Bull's-eye polar maps corresponding to data of Figure 3.

control group. To our knowledge, with these inclusion criteria, ours is the first report on nonuniform AC using an external scanning line source in ^{201}Tl SPECT instead of ^{99m}Tc-sestamibi SPECT (*29*).

The specificity of data uncorrected for attenuation appeared low in our study. This low specificity may be explained by the methodology of the protocol. The data of both groups were mixed, identification was removed, and the interpreters were unaware of any other information. A thallium scan was considered positive when any inferior defect was found. Other parameters, such as the presence of risk factors; the occurrence of chest pain; the results of electrocardiography; the size, intensity, and location of the defect; and anatomic properties of the subject (e.g., obesity), were not considered. This rough interpretation is not clinically relevant for the daily diagnosis of CAD but was necessary for a comparative evaluation of each correction method. Therefore, the low specificity we reported with FBP alone should not be considered representative of daily MPI capability.

Use of depth-dependent RR alone in phantom studies has enhanced image contrast, increasing cavity-to-wall ratio by approximately 25% without degrading the interpretation of myocardium perfusion (*30*). In our study, the accuracy of MPI was not significantly altered when RR was used. Particularly, no overestimation of inferior tracer uptake was observed. Therefore, AC seems to be responsible for the poor results obtained with the combination AC + RR. This algorithm overcorrects inferior uptake, underdetecting patients with CAD and then leading to both improved specificity and an improved normalcy rate by way of an excessive decrease in sensitivity. This pitfall was clear in patients with old documented inferior infarction without evidence of myocardial viability.

The second important negative result is the creation of true apical artifacts, as occurred in 21% of the subjects (Fig. 2). This result, previously reported for a phantom study showing a significant, 15%, decrease in apical counts (*30*), applies to humans too. Some authors have suggested that the generated apical defect might represent either true ischemia or physiologic thinning of the apex (*18*,*31*). This hypothesis does not agree with the characteristics of our population, in which no disease of the LAD was present. Furthermore, the analysis of our echocardiographic data showed a systolic apical thickening, rather than any thinning, in subjects free from anterior myocardial infarction. Previous studies suggested that these artifacts were generated by a relative overestimation of inferior and septal tracer uptake rather than by an underestimation of anterior or apical uptake (*32*,*33*). This overestimation could be more intense in cases of excessive bowel activity, explaining the high occurrence of this artifact in redistribution images.

Scatter correction (PER) tends to decrease the overcorrection generated by AC + RR (Fig. 3) and to restore the size of the defect and the perfusion score obtained with AC + RR to the values obtained with FBP alone. This effect is probably related to the creation of a more accurate attenuation map (*32*,*34*). These corrections also contribute to a decrease in the scattered photons from adjacent intact myocardium and abdominal organs, allowing detection of slightly injured myocardium.

Again, this effect was clear in patients with previous inferior myocardial infarction. Overestimation of myocardial viability dropped from 73% to 29% in these patients. However, the threshold of tracer uptake that we used to determine myocardial viability, which was concordant with visual analysis of the slices, was established in studies using uncorrected data. If further AC + RR correction proves of value for the positive diagnosis of CAD, further studies may be necessary to specifically address the optimum threshold. However, although the incidence of apical reverse redistribution was reduced, the final diagnostic accuracy from use of AC + RR remained unchanged. The possibility that attenuation and scatter correction are more accurate with ^{99m}Tc-MIBI than with ^{201}Tl remains controversial and has to be specifically addressed (*28*,*34*,*35*).

This study had several limitations. Only 33 subjects were processed with PER, and a more extensive study would better confirm these results. Also, the transmission CT images were not corrected for scatter because the software did not have this capability. Although this uncorrected procedure was previously validated (*9*), the precision of the μ-map might be decreased, leading to less reliable scatter correction. Further studies to evaluate the incremental accuracy that scatter correction of the transmission images provides could be helpful. Finally, our results were clearly dependent on our acquisition methodology and processing

software. Particularly, other iterative algorithms for AC might generate more accurate results.

CONCLUSION

This study showed that the combination of an AC algorithm using an external scanning line source and depth-dependent RR improved the specificity of the diagnosis of RC or Cx disease at the cost of a significant decrease in sensitivity. Moreover, besides the generation of anteroapical artifacts, this combination may induce a false-positive diagnosis of myocardial viability in cases of previous myocardial infarction. The loss of sensitivity is not restored by scatter correction, although overestimation of tracer uptake in the inferior wall is partially corrected and the number of false anteroapical reverse redistributions is reduced. The only positive effect of scatter correction that may have a clinical impact is a decrease in the number of false-positive diagnoses of viable myocardium. The reasons for the errors in estimating true inferior counts are probably multiple, and further work will be necessary to obtain good nonuniform AC without creation of artifacts.

REFERENCES

1. DePuey EG III. How to detect and avoid myocardial perfusion SPECT artifacts. *J Nucl Med.* 1994;35:699–702.
2. Rigo P, Van Boxem P, Foulon J, Safi M, Engdahl J, Links J. Quantitative evaluation of a comprehensive motion, resolution, and attenuation correction program: initial experience. *J Nucl Cardiol.* 1998;5:458–468.
3. Vanzetto G, Ormezzano O, Fagret D, Comet M, Denis B, Machecourt J. Long-term additive prognostic value of thallium-201 myocardial perfusion imaging over clinical and exercise stress test in low to intermediate risk patients: study in 1137 patients with 6-year follow-up. *Circulation.* 1999;100:1521–1527.
4. Panza JA, Dilsizian V, Laurienzo JM, Curiel RV, Katsiyiannis PT. Relation between thallium uptake and contractile response to dobutamine: implications regarding myocardial viability in patients with chronic coronary artery disease and left ventricular dysfunction. *Circulation.* 1995;91:990–998.
5. Dilsizian V, Freedman NM, Bacharach SL, Perrone-Filardi P, Bonow RO. Regional thallium uptake in irreversible defects: magnitude of change in thallium activity after reinjection distinguishes viable from nonviable myocardium. *Circulation.* 1992;85:627–634.
6. Diamond GA, Forrester JS. Analysis of probability as an aid in the clinical diagnosis of coronary-artery disease. *N Engl J Med.* 1979;300:1350–1358.
7. Daou D, Le Guludec D, Faraggi M, et al. Nonlimited exercise test combined with high-dose dipyridamole for thallium-201 myocardial single-photon emission computed tomography in coronary artery disease. *Am J Cardiol.* 1995;76:753–758.
8. Hannequin PP, Mas JF. Photon energy recovery: a method to improve the effective energy resolution of gamma cameras. *J Nucl Med.* 1998;39:555–562.
9. Bailey DL, Allen S, Cook G, Maisey M. Simultaneous emission/transmission myocardial perfusion imaging with ^{201}Tl and ^{153}Gd scanning line source: cross-over corrections and validation [abstract]. *J Nucl Med.* 1998;38(suppl):213P.
10. Formiconi AR, Pupi A, Passeri A. Compensation of spatial system response in SPECT with conjugate gradient reconstruction technique. *Phys Med Biol.* 1989; 34:69–84.
11. Liu L, Cullom SJ, White ML. A modified Weiner filter method for nonstationary resolution recovery with scatter and iterative attenuation correction for cardiac SPECT [abstract]. *J Nucl Med.* 1996;37(suppl):210P.
12. Gilland DR, Jaszczak RJ, Greer KL, Coleman RE. Quantitative SPECT reconstruction of iodine-123 data. *J Nucl Med.* 1991;32:527–533.
13. Tsui BM, Gullberg GT, Edgerton ER, et al. Correction of nonuniform attenuation in cardiac SPECT imaging. *J Nucl Med.* 1989;30:497–507.
14. Goris ML, Boudier S, Briandet PA. Two dimensional mapping of three dimensional SPECT data: a preliminary step to the quantitation of thallium myocardial perfusion single photon emission tomography. *Am J Physiol Imaging.* 1987;2: 176–180.
15. Faraggi M, Karila-Cohen D, Brochet E, et al. Relationship between resting ^{201}Tl reverse redistribution, microvascular perfusion, and functional recovery in acute myocardial infarction. *J Nucl Med.* 2000;41:393–399.
16. Holly TA, Parker JA, Hendel RC. The prevalence of non-uniform soft tissue attenuation in myocardial SPECT perfusion imaging and the impact of gated SPECT [abstract]. *J Nucl Cardiol.* 1997;49(suppl):S103.
17. Desmarais RL, Kaul S, Watson DD, Beller GA. Do false positive thallium-201 scans lead to unnecessary catheterization? Outcome of patients with perfusion defects on quantitative planar thallium-201 scintigraphy. *J Am Coll Cardiol.* 1993;21:1058–1063.
18. Ficaro EP, Fessler JA, Ackermann RJ, Rogers WL, Corbett JR, Schwaiger M. Simultaneous transmission-emission thallium-201 cardiac SPECT: effect of attenuation correction on myocardial tracer distribution. *J Nucl Med.* 1995;36:921–931.
19. Manglos SH, Bassano DA, Thomas FD. Cone-beam transmission computed tomography for nonuniform attenuation compensation of SPECT images. *J Nucl Med.* 1991;32:1813–1820.
20. Chang W, Loncaric S, Huang G, Sanpitak P. Asymmetric fan transmission CT on SPECT systems. *Phys Med Biol.* 1995;40:913–928.
21. Frey EC, Tsui BM, Perry JR. Simultaneous acquisition of emission and transmission data for improved thallium-201 cardiac SPECT imaging using a technetium-99m transmission source. *J Nucl Med.* 1992;33:2238–2245.
22. Tung C-H, Gullberg GT, Zeng GL, Christian PE, Datz FL, Morgan HT. Non-uniform attenuation correction using simultaneous transmission and emission converging tomography. *IEEE Trans Nucl Sci.* 1992;39:1134–1143.
23. Jaszczak RJ, Gilland DR, Hanson MW, Jang S, Greer KL, Coleman RE. Fast transmission CT for determining attenuation maps using a collimated line source, rotatable air-copper-lead attenuators and fan-beam collimation. *J Nucl Med.* 1993;34:1577–1586.
24. Cao Z, Tsui BM. Performance characteristics of transmission imaging using a uniform sheet source with parallel-hole collimation. *Med Phys.* 1992;19:1205–1212.
25. Hashimoto J, Ogawa K, Kubo A, et al. Application of transmission scan-based attenuation compensation to scatter-corrected thallium-201 myocardial single-photon emission tomographic images. *Eur J Nucl Med.* 1998;25:120–127.
26. Tan P, Bailey DL, Meikle SR, Eberl S, Fulton RR, Hutton BF. A scanning line source for simultaneous emission and transmission measurements in SPECT. *J Nucl Med.* 1993;34:1752–1760.
27. Hendel RC, Berman DS, Cullom SJ, et al. Multicenter clinical trial to evaluate the efficacy of correction for photon attenuation and scatter in SPECT myocardial perfusion imaging. *Circulation.* 1999;99:2742–2749.
28. Lee DS, So Y, Cheon GJ, et al. Limited incremental diagnostic values of attenuation-noncorrected gating and ungated attenuation correction to rest/stress myocardial perfusion SPECT in patients with an intermediate likelihood of coronary artery disease. *J Nucl Med.* 2000;41:852–859.
29. Kluge R, Sattler B, Seese A, Knapp WH. Attenuation correction by simultaneous emission-transmission myocardial single-photon emission tomography using a technetium-99m-labelled radiotracer: impact on diagnostic accuracy. *Eur J Nucl Med.* 1997;24:1107–1114.
30. Génin R, Daou D, Delahaye N, et al. Are attenuation correction and resolution recovery alone enough for thallium 201 SPECT studies? [abstract]. *Eur J Nucl Med.* 1999;26:1065.
31. Gallowitsch HJ, Sykora J, Mikosch P, et al. Attenuation-corrected thallium-201 single-photon emission tomography using a gadolinium-153 moving line source: clinical value and the impact of attenuation correction on the extent and severity of perfusion abnormalities. *Eur J Nucl Med.* 1998;25:220–228.
32. King MA, Xia W, deVries DJ, et al. A Monte Carlo investigation of artifacts caused by liver uptake in single-photon emission computed tomography perfusion imaging with technetium 99m-labeled agents. *J Nucl Cardiol.* 1996;3:18–29.
33. Savi A, Rossetti C, Gilardi MC, et al. Correction measured by attenuation in tomographic heart studies with single photon emission with thallium 201: comparison with positron-emission tomographic studies with ammonium marked with nitrogen [in Italian]. *Radiol Med (Torino).* 1999;98:36–42.
34. Ficaro EP, Fessler JA, Shreve PD, Kritzman JN, Rose PA, Corbett JR. Simultaneous transmission/emission myocardial perfusion tomography: diagnostic accuracy of attenuation-corrected ^{99m}Tc-sestamibi single-photon emission computed tomography. *Circulation.* 1996;93:463–473.
35. Matsunari I, Boning G, Ziegler SI, et al. Attenuation-corrected rest thallium-201/stress technetium 99m sestamibi myocardial SPECT in normals. *J Nucl Cardiol.* 1998;5:48–55.